REAL-TIME FEEDFORWARD TORQUE CONTROL OF AN INDUSTRIAL ROBOT BASED ON THE DYNAMICS MODEL

Zhang TIE[1],Liang Xiao HONG[2], Kang Zhong QIANG[3], Gong Wen TAO[4]

In the abstract, two types of real-time feedforward torque control methods (i.e., complete compensation and gravity compensation) are studied to accomplish high-precision control of an industrial robot in high-speed movement after identifying the robot's kinetic parameters. The real-time robot control platform is constructed, and the two types of feedforward torque control methods are compared with the commonly used independent PD feedback control methods through simulations and experiments. Under the complete compensation feedforward torque control method, the robot has the fastest response speed, the joint trajectory tracking error and jitter are the lowest, and the robot impact and vibration after stopping decreased more than the two other control methods. The complete compensation feedforward torque control method can be applied to the high-speed and high-precision real-time control of 6-DOF industrial robots.

Keywords: Industrial robot; Feedforward torque control; Interpolation; Complete compensation; Gravity compensation

1. Introduction

When an industrial robot (hereinafter referred to as the robot) runs in a high-speed environment, its complex nonlinearity, time-varying uncertainty, and strong coupling characteristics are extremely evident, which can seriously affect the robot motion control accuracy. The robot's servomotors must have sufficient force and torque to drive the connecting rods and joints of the robot, as well as ensure that it moves at the desired speed and acceleration. If the traditional independent PID feedback control [1-5] is used, the rods may affect the robot's localization and trajectory tracking accuracy due to the slow motion. Therefore,

[1] Prof., Dept.of Mechanical Engineering, South China University of Technology, China, e-mail: merobot@scut.edu.cn
[2]Doctor of Mechanical Engineering, South China University of Technology, China,e-mail: 348147093@qq.com
[3]Master of Mechanical Engineering, South China University of Technology, China,e-mail: 1329087575@qq.com
[4]Master of Mechanical Engineering, South China University of Technology, China,e-mail: gongwt90@126.com

establishing an accurate dynamics model and realizing the real-time control of the robot based on the dynamics model is necessary.

The control method based on the dynamics model is commonly utilized in the high-speed and high-precision motion control of the robot. The current research mainly focuses on the feedforward torque control and computed torque control method.

Feedforward torque control mainly includes two aspects: gravity compensation feedforward torque control (hereinafter referred to as gravity compensation control) and complete compensation feedforward torque control (hereinafter referred to as complete compensation control). The gravity compensation control calculates the torque term of the gravity of each joint based on the dynamics model in real time when the robot moves in accordance with the theoretical trajectory. It then adds this torque to the current loop of the servo motor as the feed torque motor. This method is easy to calculate and has a suitable control effect in the condition where the gravity term plays a dominant role in the dynamic model. In [6], a feedforward torque control method of industrial robot based on gravity compensation PID control is studied. This method has a better trajectory control effect in the robot motion with more obvious gravity work. In[7] the gravity term of the joint driving torque is calculated in real time as the compensation of the feedback torque, which can meet the requirement of the fixed point control. Liu, D. J.[8] employed the invariant gravity term as the torque feedforward, which can improve the robot's trajectory control precision by simple calculation.

Complete compensation control is more complex than gravity compensation control. It should consider the inertia force, gravity, Coriolis and centrifugal forces, and friction force of the robot dynamics model. The friction torque can reach 30% to 40% in the entire joint drive torque of the robot, so the control accuracy of the complete compensation control is higher than that of the gravity compensation control. Ruderman M. et al. [9] studied the estimation of the joint torque values of a flexible robot through the inverse kinematics model and joint structure, added it as the feedforward compensation torque value of each joint, and obtained suitable control results. Li Jin-Song et al. [10] attempted to establish the robot dynamics model in MATLAB and introduced the inertia feedforward control. Their simulation analysis shows that the control performance of the system has been improved.

The computed torque method calculates the theoretical torque of each joint based on the theoretical trajectory of the robot and then adds it into the current loop of servo motor directly; the robot motors works in the torque control mode in this case[11-13]. Veer S. et al. [14] adopted the computed torque method to compensate for the heavy torque and friction torque and realized the zero force control of the robot. The torque control of the servo motor in the torque control

mode is generally difficult to attain because the torque refresh cycle of this mode can reach the microsecond level. Control precision relies on the high precision of robot dynamics identification.

Gravity compensation control calculation is simple in the aforementioned dynamic control method. However, in several instances, the robot motion control precision can be low, the complete compensation control calculation can be more complex, and the control precision is higher. The calculation process of the computed torque method is also accurate but difficult to apply to the real-time control of robot.

This study examines two models based on the dynamics control methods for 6-DOF industrial robots (i.e., gravity compensation control and complete compensation control. The interpolation dynamics buffer queue is established, and the angle velocity and angle acceleration of each joint of the robot are computed in real time by the quintic polynomial central difference method to realize the real-time control and simplify the calculation of the feedforward torque control. The independent PID feedback control method, which has been frequently used in the robot control system, is also studied to reinforce the contrast. Finally, the aforementioned control methods are compared and verified on the real-time robot control platform.

2. Independent PID control

PID control is a typical method for the independent control of each joint. It calculates the input of the current loop of each joint according to the position error (i.e., tracking error) of the robot motor and feedback expression of the PID. The integral coefficient $\boldsymbol{K}_i$ is often set at 0. Thus, this control method is also called independent PD control. The block diagram of the independent PD control is shown in Fig.1,whose expression is presented as follows:

$$\boldsymbol{\tau}_{feedback} = \boldsymbol{K}_p(\boldsymbol{q}^* - \boldsymbol{q}) + \boldsymbol{K}_d(\dot{\boldsymbol{q}}^* - \dot{\boldsymbol{q}}) \tag{1}$$

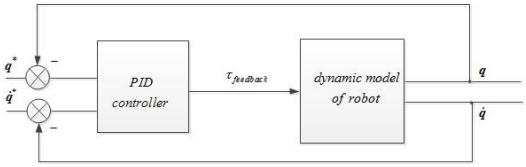

Fig. 1. System diagram of the independent PID control.

where $\boldsymbol{K}_p$ and $\boldsymbol{K}_d$ are the constant and differential coefficient matrixes for each joint of the robot, $\boldsymbol{q}^*$ is the theoretical angle of each joint, $\boldsymbol{q}$ is the actual angle of the robot, and $\dot{\boldsymbol{q}}^*$ and $\dot{\boldsymbol{q}}$ are the theoretical and actual joint angle velocities of each joint of the robot, respectively. Independent PD control is a type of PD expression, wherein all types of uncertain factors (e.g., robot parameter errors, joint friction, and external disturbances) are unified in the robot and can meet the requirements

of robot fixed-point control.

The stability criterion of the independent PD control fixed-point control is based on the following:

When ignoring the effects of gravity and friction, the dynamics expression equations of the robot with independent PD control is as presented follows:

$$\boldsymbol{M}(\boldsymbol{q})\ddot{\boldsymbol{q}}+\boldsymbol{C}(\boldsymbol{q},\dot{\boldsymbol{q}})\dot{\boldsymbol{q}}=\boldsymbol{\tau}=\boldsymbol{K}_p\boldsymbol{e}+\boldsymbol{K}_d\dot{\boldsymbol{e}} \tag{2}$$

where $\boldsymbol{M}(\boldsymbol{q})$ is an $N\times N$ order mass vector, $\boldsymbol{C}(\boldsymbol{q},\dot{\boldsymbol{q}})$ is an $N\times N$ order Coriolis force and centrifugal force vector, and N is the robot's degree of freedom. When the robot utilizes the fixed-point control, the joint angle of the robot $\boldsymbol{q}^*$ is constant, (i.e., $\dot{\boldsymbol{q}}^*=\ddot{\boldsymbol{q}}^*\equiv 0$), $\boldsymbol{e}$ is the trajectory tracking error of each joint, and $\boldsymbol{e}=\boldsymbol{q}^*-\boldsymbol{q}$. Eq.(2) can then be rewritten as follows:

$$\boldsymbol{M}(\boldsymbol{q})(\ddot{\boldsymbol{q}}^*-\ddot{\boldsymbol{q}})+\boldsymbol{C}(\boldsymbol{q},\dot{\boldsymbol{q}})(\dot{\boldsymbol{q}}^*-\dot{\boldsymbol{q}})+\boldsymbol{K}_p\,\boldsymbol{e}+\boldsymbol{K}_d\,\dot{\boldsymbol{e}}=0 \tag{3}$$

Then:

$$\boldsymbol{M}(\boldsymbol{q})\ddot{\boldsymbol{e}}+C(\boldsymbol{q},\dot{\boldsymbol{q}})\dot{\boldsymbol{e}}+\boldsymbol{K}_p\boldsymbol{e}=-\boldsymbol{K}_d\dot{\boldsymbol{e}} \tag{4}$$

The Lyapunov function is set as follows:

$$V=\frac{1}{2}\dot{\boldsymbol{e}}^T\boldsymbol{M}(\boldsymbol{q})\dot{\boldsymbol{e}}+\frac{1}{2}\boldsymbol{e}^T\boldsymbol{K}_p\boldsymbol{e} \tag{5}$$

Given that the $\boldsymbol{M}$ and $\boldsymbol{K}_p$ matrixes are positive definite matrices, then V is a globally positive definite. Thus:

$$\dot{V}=\dot{\boldsymbol{e}}^T\boldsymbol{M}\ddot{\boldsymbol{e}}+\frac{1}{2}\dot{\boldsymbol{e}}^T\dot{\boldsymbol{M}}\dot{\boldsymbol{e}}+\dot{\boldsymbol{e}}^T\boldsymbol{K}_p\boldsymbol{e} \tag{6}$$

Given the robot's property (i.e., the skew symmetry of the $\dot{\boldsymbol{M}}-2\boldsymbol{C}$ matrix), Eq.(6)can be rewritten as follows:

$$\begin{aligned}\dot{V}&=\dot{\boldsymbol{e}}^T\boldsymbol{M}\ddot{\boldsymbol{e}}+\frac{1}{2}\dot{\boldsymbol{e}}^T\dot{\boldsymbol{M}}\dot{\boldsymbol{e}}+\dot{\boldsymbol{e}}^T\boldsymbol{K}_p\dot{\boldsymbol{e}}\\&=\dot{\boldsymbol{e}}^T(\boldsymbol{M}\ddot{\boldsymbol{e}}+C\dot{\boldsymbol{e}}+\boldsymbol{K}_p\boldsymbol{e})=-\dot{\boldsymbol{e}}^T\boldsymbol{K}_d\dot{\boldsymbol{e}}\le 0\end{aligned} \tag{7}$$

Eq.(7) shows that $\dot{V}$ is a negative semi-definite, whereas $\boldsymbol{K}_d$ is a positive definite matrix. $\dot{\boldsymbol{e}}\equiv 0$ would then be certainly correct when $\dot{V}\equiv 0$,which is then added to Eq.(4) (i.e., $\boldsymbol{K}_p\boldsymbol{e}=0$). Given LaSalle's invariance theorem, $(\boldsymbol{e},\dot{\boldsymbol{e}})=(\boldsymbol{0},\boldsymbol{0})$ is an asymptotically stable equilibrium point of the robot. $\boldsymbol{q}\to\boldsymbol{q}_d,\dot{\boldsymbol{q}}\to\boldsymbol{0}$ can then be finally obtained from the arbitrary initial conditions $(\boldsymbol{q}_0,\dot{\boldsymbol{q}}_0)$, so the point control of the robot based on independent PD control can be accomplished.

3. Real-time feedforward torque control based on the dynamics model

Feedforward torque control based on the dynamics model is calculated based on the motion theoretical trajectory and identified inverse dynamics model of the robot. The real-time interpolation of the robot calculates the theoretical driven joint torque of its desired trajectory. The theoretical driving torque and PD feedback interaction torque would then be combined and placed in the current loop of every servo motor. The theoretical driving torque is called the feedforward compensation torque. In the case of the accurate robot dynamics model, the trajectory tracking accuracy is higher than that of the independent PD control. The system diagram of the feedforward torque control method based on the dynamics model is shown in Fig.2.

The feedforward compensation torque in the control block diagram is calculated as follows:

$$\boldsymbol{\tau}_{feedforward} = \boldsymbol{H}_b(\boldsymbol{q}^*, \dot{\boldsymbol{q}}^*, \ddot{\boldsymbol{q}}^*) \bullet \boldsymbol{\beta} \tag{8}$$

The equation for calculating the feedback torque is as follows:

$$\boldsymbol{\tau}_{feedback} = \boldsymbol{K}_p(\boldsymbol{q}^* - \boldsymbol{q}) + \boldsymbol{K}_d(\dot{\boldsymbol{q}}^* - \dot{\boldsymbol{q}}) \tag{9}$$

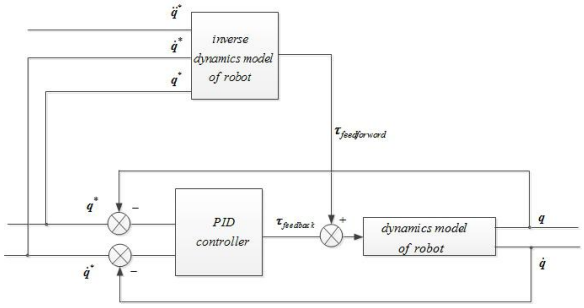

Fig. 2. System diagram of the feedforward torque control.

In Equation (8), $\boldsymbol{\tau}_{feedforward}$ is the feedforward torque calculated based on the inverse dynamics model, joint angle $\boldsymbol{q}^*$, joint angle velocity $\dot{\boldsymbol{q}}^*$, and joint angle acceleration $\ddot{\boldsymbol{q}}^*$. $\boldsymbol{q}$ and $\dot{\boldsymbol{q}}$ are the actual joint angle and actual joint velocity of each joint, respectively, when the robot is actually running.

The feedforward torque control based on the dynamic model is the combination of the feedforward compensation torque and feedback torque. It acts on the bottom of the servo motor as the compensation of the current loop. The torque expression is as follows:

$$\boldsymbol{\tau} = \boldsymbol{\tau}_{feedback} + \boldsymbol{\tau}_{feedfoward} \tag{10}$$

where the feedforward torque $\boldsymbol{\tau}_{feedforward}$ provides the joint driving torque required to attain the desired motion of the joint, whereas the PD feedback torque $\boldsymbol{\tau}_{feedback}$

compensates for the unknown external disturbances and non-model forces of the system.

The feedforward torque control can be divided into two types: gravity compensation control, in which the $\boldsymbol{\tau}_{feedforward}$ only includes gravity torque, and complete compensation control, in which the $\boldsymbol{\tau}_{feedforward}$ includes inertial force, gravity, Coriolis and centrifugal forces, and friction force.

3.1 Gravity compensated feedforward torque control

When gravity compensation control is used, the feedforward torque $\boldsymbol{\tau}_{feedforward}$ is calculated based on the dynamics model of the robot as follows:

$$\boldsymbol{\tau}_{feedforward} = \boldsymbol{G}(\boldsymbol{q}^*) \tag{11}$$

The combined torque is then expressed as follows:

$$\boldsymbol{\tau} = \boldsymbol{G}(\boldsymbol{q}^*) + \boldsymbol{K}_p(\boldsymbol{q}^* - \boldsymbol{q}) + \boldsymbol{K}_d(\dot{\boldsymbol{q}}^* - \dot{\boldsymbol{q}}) \tag{12}$$

For the N-DOF robot, its dynamics equation is similarly expressed as follows:

$$\begin{aligned} &\boldsymbol{M}(\boldsymbol{q})\ddot{\boldsymbol{q}} + \boldsymbol{C}(\boldsymbol{q},\dot{\boldsymbol{q}})\dot{\boldsymbol{q}} + \boldsymbol{G}(\boldsymbol{q}) = \boldsymbol{\tau} \\ &= \boldsymbol{G}(\boldsymbol{q}^*) + \boldsymbol{K}_p(\boldsymbol{q}^* - \boldsymbol{q}) + \boldsymbol{K}_d(\dot{\boldsymbol{q}}^* - \dot{\boldsymbol{q}}) \end{aligned} \tag{13}$$

The equation can be changed into the following:

$$\boldsymbol{M}(\boldsymbol{q})\ddot{\boldsymbol{e}} + \boldsymbol{C}(\boldsymbol{q},\dot{\boldsymbol{q}})\dot{\boldsymbol{e}} + \boldsymbol{K}_p\boldsymbol{e} + \boldsymbol{K}_d\dot{\boldsymbol{e}} + \boldsymbol{G}(\boldsymbol{q}^*) - \boldsymbol{G}(\boldsymbol{q}) = \boldsymbol{0} \tag{14}$$

In the case of the accurate robot dynamics model, $\boldsymbol{G}(\boldsymbol{q}^*) = \boldsymbol{G}(\boldsymbol{q})$ would hold, and then Eq.(14) can be changed to the following:

$$\boldsymbol{M}(\boldsymbol{q})\ddot{\boldsymbol{e}} + (\boldsymbol{C}(\boldsymbol{q},\dot{\boldsymbol{q}}) + \boldsymbol{K}_d)\dot{\boldsymbol{e}} + \boldsymbol{K}_p\boldsymbol{e} = \boldsymbol{0} \tag{15}$$

At this point, the stability is similar to that of the independent PD control. The gravity compensation feedforward torque control can realize the fixed-point control of the robot.

3.2 Complete compensation feedforward torque control

When complete torque control is utilized, the feedforward torque $\boldsymbol{\tau}_{feedforward}$ is calculated based on the dynamics model of the robot as follows:

$$\boldsymbol{\tau}_{feedforward} = \boldsymbol{M}(\boldsymbol{q}^*)\ddot{\boldsymbol{q}}^* + \boldsymbol{C}(\boldsymbol{q}^*,\dot{\boldsymbol{q}}^*)\dot{\boldsymbol{q}}^* + \boldsymbol{G}(\boldsymbol{q}^*) + \boldsymbol{F}(\dot{\boldsymbol{q}}^*) \tag{16}$$

where $\boldsymbol{M}(\boldsymbol{q}^*)\ddot{\boldsymbol{q}}^*$ is the inertial force term in the robot dynamics model, $\boldsymbol{C}(\boldsymbol{q}^*,\dot{\boldsymbol{q}}^*)\dot{\boldsymbol{q}}^*$ is the Coriolis and centrifugal forces term, $\boldsymbol{G}(\boldsymbol{q}^*)$ is the gravity term, and $\boldsymbol{F}(\dot{\boldsymbol{q}}^*)$ is the friction force.

In rotating machines, motors, and gears, a relationship exists between the friction force and rotation speed. In this paper, the improved friction model is used[15].

When complete compensation control is employed, the combined torque is

calculated from the following:

$$\begin{aligned}\boldsymbol{\tau} &= \boldsymbol{M}(\boldsymbol{q}^*)\ddot{\boldsymbol{q}}^* + \boldsymbol{C}(\boldsymbol{q}^*, \dot{\boldsymbol{q}}^*)\dot{\boldsymbol{q}}^* + \boldsymbol{G}(\boldsymbol{q}^*) + \boldsymbol{F}(\dot{\boldsymbol{q}}^*) \\ &+ \boldsymbol{K}_p(\boldsymbol{q}^* - \boldsymbol{q}) + \boldsymbol{K}_d(\dot{\boldsymbol{q}}^* - \dot{\boldsymbol{q}})\end{aligned} \tag{17}$$

For the N-DOF robot, its inverse dynamics equation is similarly presented as follows:

$$\begin{aligned}\boldsymbol{\tau} &= \boldsymbol{M}(\boldsymbol{q}^*)\ddot{\boldsymbol{q}}^* + \boldsymbol{C}(\boldsymbol{q}^*, \dot{\boldsymbol{q}}^*)\dot{\boldsymbol{q}}^* + \boldsymbol{G}(\boldsymbol{q}^*) + \boldsymbol{F}(\dot{\boldsymbol{q}}^*) \\ &+ \boldsymbol{K}_p(\boldsymbol{q}^* - \boldsymbol{q}) + \boldsymbol{K}_d(\dot{\boldsymbol{q}}^* - \dot{\boldsymbol{q}}) \\ &= \boldsymbol{M}(\boldsymbol{q})\ddot{\boldsymbol{q}} + \boldsymbol{C}(\boldsymbol{q}, \dot{\boldsymbol{q}})\dot{\boldsymbol{q}} + \boldsymbol{G}(\boldsymbol{q}) + \boldsymbol{F}(\dot{\boldsymbol{q}})\end{aligned} \tag{18}$$

Equation (18) can be changed to the following:

$$\begin{aligned}&\boldsymbol{K}_p\boldsymbol{e} + \boldsymbol{K}_d\dot{\boldsymbol{e}} + (\boldsymbol{M}(\boldsymbol{q}^*) - \boldsymbol{M}(\boldsymbol{q}))\ddot{\boldsymbol{q}}^* + \\ &(\boldsymbol{C}(\boldsymbol{q}^*, \dot{\boldsymbol{q}}^*) - \boldsymbol{C}(\boldsymbol{q}, \dot{\boldsymbol{q}}))\dot{\boldsymbol{q}}^* + \boldsymbol{M}(\boldsymbol{q})\ddot{\boldsymbol{e}} + \\ &\boldsymbol{C}(\boldsymbol{q}, \dot{\boldsymbol{q}})\dot{\boldsymbol{e}} + (\boldsymbol{G}(\boldsymbol{q}^*) - \boldsymbol{G}(\boldsymbol{q})) + \\ &\boldsymbol{F}(\dot{\boldsymbol{q}}^*) - \boldsymbol{F}(\dot{\boldsymbol{q}}) = \boldsymbol{0}\end{aligned} \tag{19}$$

In Eq. (19), set

$$\begin{aligned}\boldsymbol{h} &= (\boldsymbol{M}(\boldsymbol{q}^*) - \boldsymbol{M}(\boldsymbol{q}))\ddot{\boldsymbol{q}}^* + (\boldsymbol{C}(\boldsymbol{q}^*, \dot{\boldsymbol{q}}^*) - \boldsymbol{C}(\boldsymbol{q}, \dot{\boldsymbol{q}}))\dot{\boldsymbol{q}}^* \\ &+ (\boldsymbol{G}(\boldsymbol{q}^*) - \boldsymbol{G}(\boldsymbol{q})) + \boldsymbol{F}(\dot{\boldsymbol{q}}^*) - \boldsymbol{F}(\dot{\boldsymbol{q}})\end{aligned} \tag{20}$$

Equation (19) can then be changed to the following:

$$\boldsymbol{K}_p\boldsymbol{e} + \boldsymbol{K}_d\dot{\boldsymbol{e}} + \boldsymbol{h} + \boldsymbol{M}(\boldsymbol{q})\ddot{\boldsymbol{e}} + \boldsymbol{C}(\boldsymbol{q}, \dot{\boldsymbol{q}})\dot{\boldsymbol{e}} = \boldsymbol{0} \tag{21}$$

In Santibañez, V., andKelly, R.'s theory[16], the Lyapunov function was established based on Eq.(18) and Eq.(21) . This function proves that in the case of selecting the proper PD coefficient matrices $\boldsymbol{K}_p$ and $\boldsymbol{K}_d$, the closed-loop system is globally asymptotically stable at the atmosphere of $(\boldsymbol{e}, \dot{\boldsymbol{e}}) = (\boldsymbol{0}, \boldsymbol{0})$. It does not require the robot's joint theoretical angle $\boldsymbol{q}^*$ to be constant, so it is stable not only when the robot is in fixed-point control.

Unlike independent PD control and gravity compensation control, the complete compensation control has the following advantages:

(1) When the robot inverse dynamics model is accurate, the complete compensation feedforward torque is close to the actual torque required by the servo motor according to the theoretical trajectory of robot. Thus, the function of $\boldsymbol{\tau}_{feedback}$ and trajectory tracking error of each joint of robot decrease before the trajectory deviation occurs.

(2) The complete compensation control attains the deep effect of the inner ring of the robot's servo motor. This process is necessary to attain fast and stable servo response. It is also conducive to improve the response speed of the servo control system of robot.

(3) The traditional independent PID control method often improves the positioning accuracy of the robot by increasing the gain of the PD feedback. However, the excessive PD gain will make the robot clearly vibrate or even unstable. By contrast, a large part of the torque demand in the complete compensation feedforward torque control can be originated from the feedforward torque. Hence, the PD feedback gain can be lowered, and better control results can be obtained.

3.3 Calculation method of the real-time feedforward torque

After determining the dynamics parameters and model of the robot, we can calculate the feedforward torque based on Eq. (16). In the real-time interpolation of the robot, we can only obtain the theoretical interpolation point $\boldsymbol{q}^*$ of each joint. Thus, we should calculate the real-time theoretical joint angle velocity $\dot{\boldsymbol{q}}^*$ and theoretical angle acceleration $\ddot{\boldsymbol{q}}^*$ according to the theoretical trajectory of the robot and joint angle of every joint.

The dynamic buffer queue and the central difference method are used to calculate the joint angle velocity and angle acceleration.

If five adjacent interpolation points are known, then the joint angle velocity and joint angle acceleration of third points (middle point) can be calculated by the central difference method[17]. Differential calculation naturally has the function of noise amplification[18]. The direct forward difference of the joint rotation angle would amplify the amplitude of the high-frequency noise. It will also result in the waveform distortion of the angle velocity and angle acceleration, as well as affect the accuracy of the feedforward torque calculation.

The time interval between the five interpolation points is set at T (i.e., the theoretical interpolation period of the robot), whereas the time series of the third points is set at $\boldsymbol{q}(x)$. The time series of the other points are as follows: $\boldsymbol{q}(x-2T)$, $\boldsymbol{q}(x-T)$, $\boldsymbol{q}(x+T)$, and $\boldsymbol{q}(x+2T)$. The Taylor four-order expansions of $\boldsymbol{q}(x-2T)$, $\boldsymbol{q}(x-T)$, $\boldsymbol{q}(x+T)$, and $\boldsymbol{q}(x+2T)$ are then conducted, and the subtraction can be obtained as follows:

$$\boldsymbol{q}(x+T)-\boldsymbol{q}(x-T)=2\boldsymbol{q}'(x)T+\frac{2\boldsymbol{q}^{(3)}(x)T^3}{3!}+\frac{2\boldsymbol{q}^{(5)}(c_1)T^5}{5!} \tag{22}$$

$$\boldsymbol{q}(x+2T)-\boldsymbol{q}(x-2T)=4\boldsymbol{q}'(x)T+\frac{16\boldsymbol{q}^{(3)}(x)T^3}{3!}+\frac{64\boldsymbol{q}^{(5)}(c_2)T^5}{5!} \tag{23}$$

where c_1 and c_2 are constants, and Eq. (22) is multiplied by 8 minus Eq. (23) to obtain the following:

$$\begin{aligned} &\boldsymbol{q}(x-2T)+8\boldsymbol{q}(x+T)-8\boldsymbol{q}(x-T)-\boldsymbol{q}(x+2T) \\ &=12\boldsymbol{q}'(x)T+\frac{(16\boldsymbol{q}^{(5)}(c_1)-64\boldsymbol{q}^{(5)}(c_2))T^5}{120} \end{aligned} \tag{24}$$

Determining a constant $c\in[x-2T,x+2T]$ is always possible, which satisfies the following:

$$16\boldsymbol{q}^{(5)}(c_1)-64\boldsymbol{q}^{(5)}(c_2)=-48\boldsymbol{q}^{(5)}(c) \tag{25}$$

After sorting using types (24) and (25), the following can be obtained:

$$\begin{aligned} \boldsymbol{q}'(x)=&\frac{\boldsymbol{q}(x-2T)+8\boldsymbol{q}(x+T)-8\boldsymbol{q}(x-T)-\boldsymbol{q}(x+2T)}{12T} \\ &+\frac{\boldsymbol{q}^{(5)}(c)T^4}{30} \end{aligned} \tag{26}$$

The two-order central difference algorithm can be similarly applied to compute $\boldsymbol{q}''(x)$ as follows:

$$\begin{aligned} \boldsymbol{q}''(x)=&\frac{-\boldsymbol{q}(x+2T)+16\boldsymbol{q}(x+T)-30\boldsymbol{q}(x)}{12T^2} \\ &+\frac{16\boldsymbol{q}(x-T)-\boldsymbol{q}(x-2T)}{12T^2} \end{aligned} \tag{27}$$

The joint angle queue of the robot real-time interpolation point is $\boldsymbol{Q}$. Five points in a row from $\boldsymbol{Q}$ are taken and then added to the interpolation dynamic buffer queue $\boldsymbol{Q}_c$ as shown in Fig.3. The said figure shows that starting from the first point, five points from queue $\boldsymbol{Q}$ are taken and placed into the interpolation cache queue. The joint angle velocity and angle acceleration of the third points are then calculated. After the calculation, the first point in $\boldsymbol{Q}_c$ (tail) is removed, and then a point from queue $\boldsymbol{Q}$ (team head) is taken. The new queue $\boldsymbol{Q}_c$ is built, and then the joint angle velocity and angle acceleration of the third point of the new cache queue are calculated. This process completes the calculation until the last point of queue $\boldsymbol{Q}$ is added to the cache queue. Thus, apart from the first, the second, the last second, and the last point in the interpolation point queue $\boldsymbol{Q}$, the other theoretical joint angle velocity $\dot{\boldsymbol{q}}^*$ and joint angle acceleration $\ddot{\boldsymbol{q}}^*$ of points in queue $\boldsymbol{Q}$ have been calculated.

The second and last second points can be calculated by the central difference principle of three points:

$$\dot{\boldsymbol{q}}_2=\frac{\boldsymbol{q}_3-\boldsymbol{q}_1}{2T} \tag{28}$$

$$\ddot{\boldsymbol{q}}_2=\left(\frac{\boldsymbol{q}_3-\boldsymbol{q}_2}{T}-\frac{\boldsymbol{q}_2-\boldsymbol{q}_1}{T}\right)/T \tag{29}$$

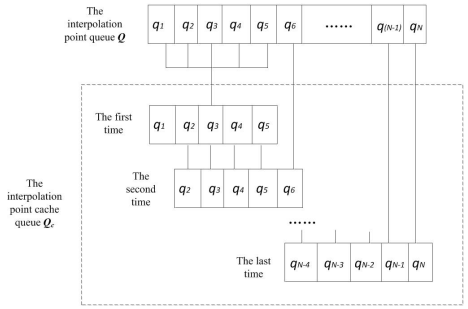

Fig. 3. Establishment of the interpolation dynamic cache queue.

$$\dot{\boldsymbol{q}}_{N-1} = \frac{\boldsymbol{q}_N - \boldsymbol{q}_{N-2}}{2T} \tag{30}$$

$$\ddot{\boldsymbol{q}}_{N-1} = \left(\frac{\boldsymbol{q}_N - \boldsymbol{q}_{N-1}}{T} - \frac{\boldsymbol{q}_{N-1} - \boldsymbol{q}_{N-2}}{T}\right) / T \tag{31}$$

For the first and last points of the interpolation point, the theoretical joint angle velocity $\dot{\boldsymbol{q}}^*$ and theoretical joint angle acceleration $\ddot{\boldsymbol{q}}^*$ cannot be obtained by the central difference. The joint angle velocity acceleration of the first and last interpolation points can be set to zero, which is equivalent to the feedforward torque of the two interpolation points that only contains the gravity terms. Given that the robot interpolation cycle is extremely short (commonly 1 ms) and the velocity and acceleration at the first and last cycles of the robot are small, only a minimal calculation error can occur.

When calculating the feedforward torque value of the gravity compensation control according to Eq. (11), establishing a dynamic cache queue and quintic polynomial central difference calculations $\dot{\boldsymbol{q}}^*$ and $\ddot{\boldsymbol{q}}^*$ is unnecessary because the gravity term is only related to the theoretical angle $\boldsymbol{q}^*$ of each joint of the robot.

Thus, we can calculate the feedforward torque in real time by using the central difference method.

4. Experimental research and analysis

4.1 Experiment platform

The experimental platform is a 6-DOF robot platform based on an open controller system to meet the real-time requirement of interpolation. 3D and 1D acceleration sensors are separately installed at the end center of load and base of the robot as shown in Fig.4.

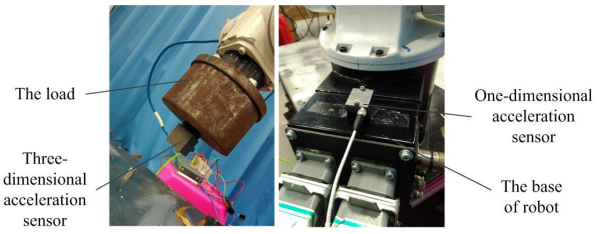

Fig. 4. Installation of the acceleration sensor

4.2 Experimental research and analysis

The coordinate system of the 6-DOF robot is established according to [19-21], and the parameters of the robot link are determined as follows: $a_1 = a_3 = d_3 = 0$ and $a_2 = d_4$ =250 mm.The Max Working Radius is 500mm. The MOA(Max Operation Area)of 6 joints are listed in Table 1. A total of 4 teaching points which are the transition points on the robot path are selected in the robot's motion space, and the experimental track is selected as a typical "gate" track in the 3C industry which requires high-speed and high-precision. The position of the teaching points is listed in Table 2.

Table1. The Max Operation Area of 6 joints

Joint	J1	J2	J3	J4	J5	J6
MOA/°	±170°	±115°	+40°~-220°	±185°	±125°	±360°

Table 2. Teaching points of the experiment on the feedforward torque control.

Points	x/mm	y/mm	z/mm	α/°	β/°	γ/ °
p_3	264.31	285.5	-54.50	73.09	-8.18	176.7
p_5	385.91	-49.44	-54.54	18.59	-8.17	176.7
p_7	186.82	187.9	260.6	79.76	-33.61	156.6
p_8	256.53	-93.1	258.47	14.42	-33.15	156.9

The center of the robot end is in the motion space of the robot, and the contrastive experiment of the gravity compensation control, complete compensation control, and independent PD control are performed. The maximum speed is set at 1,500 mm/s, tangential acceleration at 50,000 mm/s^2, and ratio of the jerk speed and acceleration of S speed planning at 50. The load mass is 3 kg, and the robot trajectory is to move straight from p_3 to p_7, then to p_8, and finally to p_5. *p3* is the starting and ending points of acceleration and *p5* is the ending point of the trajectory, *p7* and *p8* are near two right-angle points on the trajectory where the joints' output torque is obviously not enough to meet the requirements of high speed and high precision of robot.The schematic of the trajectory is shown in Fig.5.

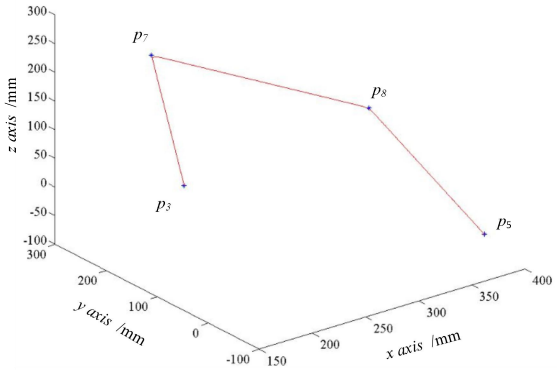

Fig. 5. Schematic of the trajectory.

In each interpolation cycle, the encoder values of each joint motor, 3D, and 1D acceleration sensor readings are read in real time to compare and analyze the data. The experimental results are compared and analyzed from the four aspects of robot response speed, encoder value change, robot tracking error of each joint trajectory, and acceleration jitter of the robot.

(1) Robot response aspect

Under the three control methods, the readings of the motor encoders are preserved in real time during the robot movement and drawn in MATLAB. The changes in the readings of the motor encoders when the robot starts are shown in Fig.6.

The said figure shows that the green curve represents the theoretical value of the motor encoder, the red curve represents the complete compensation control, the blue curve represents the gravity compensation control, and the black curve represents the independent PD control (i.e., the picture abscissa is the interpolation point sequence, whereas the ordinate is the encoder value).

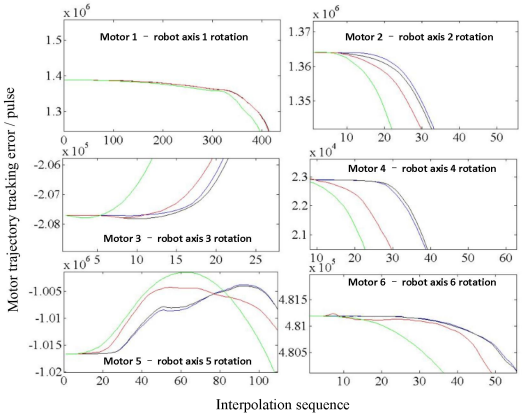

Fig. 6. Motor encoder reads when the robot starts under the three control methods.

Fig. 6.also shows that unlike the independent PD control and gravity compensation control, in the complete compensation control, the motor starting speed improved to a certain extent, the average response time of each motor

shortened by approximately 5 ms (i.e., the time interval for each interpolation point sequence is 1 ms), and the control effects of the independent PD control and gravity compensation control are similar.

(2) Trajectory tracking error of the robot joints

In the process of robot operation, we can obtain the robot motor tracking error of each interpolation cycle with the actual read value of the encoder (each interpolation cycles only reads once) minus the theoretical value of the motor encoder. Given the similarity of the independent PD control and gravity compensation control, we only compare the motor tracking errors of the gravity compensation and complete compensation, which are then drawn in the MATLAB as shown in Fig.7.

Figure 7.shows that with the use of complete compensation control, the tracking error of each motor trajectory (closer to 0 would be smaller) should be less than the use of gravity compensation control in general. The maximum tracking error can be lowered to 40% of the track. The trajectory tracking accuracy of robot can be largely improved in this approach, and the accuracy of robot motion at high speeds can be improved.

(3) Robot acceleration

The 3D and 1D acceleration sensors are installed at the end of the robot load and base. When the robot is running and within 2s after it stops, the acceleration sensor will measure the acceleration values in real time. In MATLAB, the three directions and composite acceleration values of the robot end acceleration sensors of the two methods (i.e., complete compensation and gravity compensation

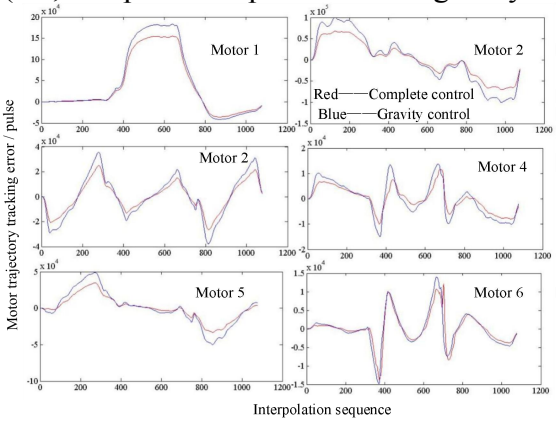

Fig. 7. Trajectory tracking error of each motor when the robot is running under the two control methods.

feedforward control) are drawn after filtering as shown in Fig.8. The acceleration difference in each direction of the two control methods is drawn in MATLAB after the robot stops to better compare the jitter of the robot end in all directions as shown in Fig.9.

Figure 8.shows that under complete compensation feed forward torque

control, the acceleration fluctuation in each direction when the direction of the robot end changes is smaller than the gravity compensation feedforward control. The peak acceleration and acceleration change are also close to the set value of the robot. Fig.9 shows that after the robot stops, the maximum amount of jitter in the X direction of the robot end decreased by 0.75 g, that in the Y direction decreased by 0.55 g, and that in the Z axis decreased by 1.5 g in complete compensation control unlike gravity compensation control.

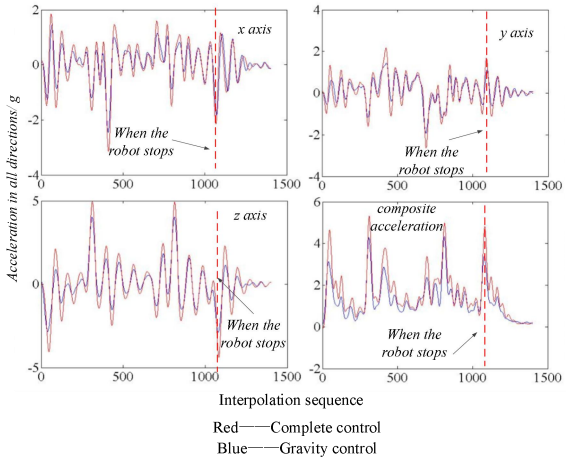

Fig. 8. Robot end acceleration under the two control methods.

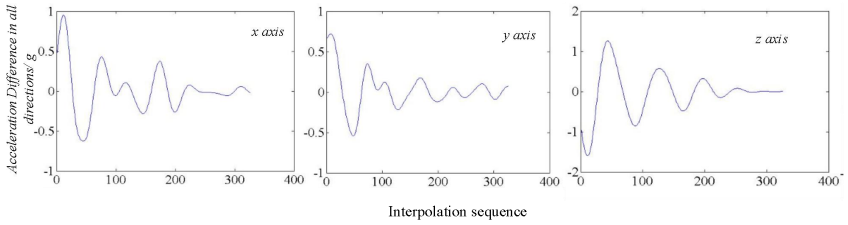

Fig. 9. Difference in acceleration after the robot stops under the two control methods.

For the base acceleration, the filtering process is not performed because the vibration of the base has a high frequency when the robot is moving. The acceleration contrast of the base under the two control methods is shown in Fig.10. The figure shows that the red line is the base acceleration of the gravity compensation control, whereas the blue line is the acceleration value of the complete compensation control.

Figure 10.shows that the vibration acceleration of the robot base under complete compensation control is smaller, the maximum high frequency vibration decreased by 51.92%, the average value of the high frequency vibration decreased by 21.37%, and the variance decreased by 37.01% unlike gravity compensation control. These results show that the shock and vibration of the robot body are much smaller than those of the gravity compensation control when the complete compensation control method is used.

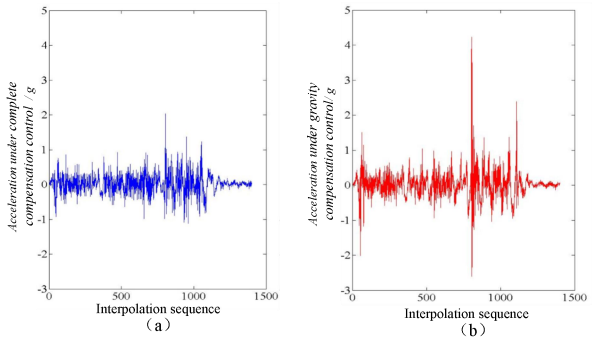

Fig. 10.(a) the base acceleration under complete compensation control (b) the base acceleration under gravity compensation control

5. Conclusions

The real-time feedforward torque control method based on the dynamics model is
examined in this study. Two feedforward torque control methods (i.e., gravity compensation and complete compensation) are analyzed. The advantages and disadvantages of the two methods are compared, and their stability levels are proved. The method of establishing the dynamic buffer queue and using the central difference method to calculate the feedforward compensation torque in real time is also studied. A real-time robot control system is built. The two types of feedforward torque and PD feedback control methods, which are commonly employed in robot control systems, are compared and analyzed. Thus, the following conclusions are obtained:

(1) When the robot is running at a high speed, the motion control effects in the gravity compensation control and PD feedback control are equivalent when these methods are applied.

(2) In complete compensation control, expected torque will be calculated based on the dynamic model and it will be compensated in the current loop, the response speed of the robot increased by approximately 5 ms, each joint vibration is less than 20% when the robot stops, the robot motor tracking error decreased by 40%, The vibration of robot end in X, Y, Z direction is reduced by 1.5g at most and 0.55g at least after the robot stops, and the maximum high frequency vibration of the robot base decreased by 51.92% unlike gravity compensation control.

REFERENCES

[1] *Riahi, A., & Balochian, S.*,Trajectory following of an industrial robot using optimized fractional order pid controller. Ijecce. 2014

[2] *Shareef, Z., & Trachtler, A.*, “Optimal trajectory planning for robotic manipulators using Discrete Mechanics and Optimal Control”. Control Applications (**Vol.82**, pp.240-245). 2014

[3] *Dehghani, A., & Khodadadi, H.* ,“Fuzzy logic self-tuning pid control for a single-link flexible joint robot manipulator in the presence of uncertainty”. 186-191. 2015

[4] *Mendoza, M., Zavala-Río, A., Santibáñez, V., & Reyes, F.*, "A generalised pid-type control scheme with simple tuning for the global regulation of robot manipulators with constrained inputs". International Journal of Control(10), 1-18. 2015

[5] *Reham, H., Bendary, F., & Elserafi, K.* , "Trajectory tracking control for robot manipulator using fractional order-fuzzy-pid controller". International Journal of Computer Applications, 134. 2016

[6] *Kelly, R., Davila, V. S., & Loría, A.* Control of Robot Manipulators in Joint Space. Springer London. 2005

[7] *Resquín, F., Gonzalez-Vargas, J., Ibáñez, J., Brunetti, F., & Pons, J. L.* ,"Feedback error learning controller for functional electrical stimulation assistance in a hybrid robotic system for reaching rehabilitation". European Journal of Translational Myology, 26(3), 6164. 2016

[8] *Liu, D. J., Tian, Y. T., & Xun, G.* ,"Control of biped robot based on energy and angle invariant combination". Journal of Shenyang University of Technology.2011

[9] *Ruderman, M., & Iwasaki, M.* ,"Control of nonlinear elastic joint robots using feed-forward torque decoupling". Ifac Papersonline, 48(11), 137-142. 2015

[10] *Jin-Song, L. I., Zhao, L. Y., & Liu, Z. Z.* ,"Research of industrial robot inertia feedforward control simulation based on matalb/simmechanics".Journal of Tianjin University of Technology. 2015

[11] *Lu, J., Haninger, K., Chen, W., & Tomizuka, M.* ,"Design and torque-mode control of a cable-driven rotary series elastic actuator for subject-robot interaction". IEEE International Conference on Advanced Intelligent Mechatronics (pp.158-164). 2015

[12] *Whitney, C. E., Bauerle, P. A., Jin, N., Shupe, T. R., & Simon, R. C.* ,"Cooridnated torque control operation with de-energized throttle".US, US9068517.2015

[13] *Ghaderi, A., Soltani, J., Ebrahimi, M., & Nassiraei, A. A. F.* ,"Modification of electric drive vehicles performances using a direct torque control with over-modulation ability". Industrial Electronics Society, IECON 2015 -, Conference of the IEEE. 2016

[14] *Daigoro Isobe,Daisaku Imaizumi,Youichi Chikugo,Shunsuke Sato* ,"A parallel solution scheme for inverse dynamics and its application in feed-forward control of link mechanisms".Journal of Robotics and Mechatronics **Vol**.15 No.1,2003.

[15] *Tie Zhang,Jingdong Hong&Xiaogang Liu*, "Dragging Teaching Method without Torque Sensor for Robot Based on Elastic Friction Model(in Chinese)" , Transactions of the Chinese Society for Agricultural Machinery, 50(1):412-419,2019.

[16] *Veer, S., Motahar, M. S., & Poulakakis, I.* ,"On the adaptation of dynamic walking to persistent external forcing using hybrid zero dynamics control". Ieee/rsj International Conference on Intelligent Robots and Systems (pp.997-1003). 2015

[17] *Santibañez, V., & Kelly, R.* ,"PD control with feedforward compensation for robot manipulators: analysis and, experimentation".Robotica, 19(1), 11-19. 2001

[18] *Gautier, M.* ,"Dynamic identification of robots with power model".IEEE International Conference on Robotics and Automation, 1997. Proceedings (**Vol**.3, pp.1922-1927 vol.3). IEEE.

[19] *Ovaska, S. J., & Valiviita, S.* ,"Angular acceleration measurement: a review". IEEE Transactions on Instrumentation & Measurement, 47(5), 1211-1217. 1998

[20] *Yang, C., Ma, H., & Fu, M.* ,"Robot Kinematics and Dynamics Modeling". Advanced Technologies in Modern Robotic Applications. Springer Singapore. 2016

[21] *Altafini, C.* Advances in Robot Kinematics: J.L. Lenarcic, M.M. Stanisic (Eds.), Kluwer Academic Publishers, Dordrecht, ISBN 0-7923-6426-0, Copyright 2000. Automatica, 2005, 41(11):2011-2012.